Articles

Penetration and Intracellular Routing of Nucleus-Directed Peptide-Based Shuttles (Loligomers) in Eukaryotic Cells†

Devender Singh, Reza Kiarash, Kim Kawamura, Eric C. LaCasse, and Jean Gariépy*

Department of Medical Biophysics, University of Toronto and Ontario Cancer Institute, Princess Margaret Hospital, 610 University Avenue, Toronto, Canada M5G 2M9

Received November 10, 1997; Revised Manuscript Received January 21, 1998

ABSTRACT: Loligomers are multitasking, peptide-based shuttles that are able to penetrate cells and self-localize into distinct cellular compartments. In particular, loligomer 4 incorporates internalization and nuclear import sequences as well as reporter groups. The intracellular routing of loligomer 4 was analyzed by microscopy and flow cytometry, to define and demonstrate localization events. Electron micrographs of CHO cells exposed to a biotinylated derivative of loligomer 4 as well as confocal images of CHO cells treated with rhodamine-labeled loligomer 4 indicate their presence in the cytosol, endocytic vesicles, and the nucleus of CHO cells. Loligomer 4 accumulates irreversibly inside cells. Uptake of loligomer 4 by six mammalian cell lines (Daudi, EL4, CHO, COS-7, VERO, and HeLa) was proven by flow cytometry, establishing the generality of the principle. Cells presented as monolayers typically were less able to endocytose the construct than cells grown in suspension. Cellular accumulation of loligomer 4 varied between cell lines with COS-7 and VERO cells showing the highest level of uptake. Plasmids harboring reporter genes could be transported efficiently inside CHO cells, suggesting that loligomer 4 either alone or noncovalently associated with large macromolecules can effectively reach the nucleus of cells. In summary, loligomer 4 constructs provide a simple synthetic platform for the design of guided intracellular agents.

The area of preclinical drug discovery presently relies on chemical and peptide libraries in conjunction with high-throughput screening approaches to dramatically shorten the time required to identify low-molecular weight lead compounds with a promising therapeutic property (*1, 2*). However, mechanisms of drug resistance and intracellular trafficking remain challenging problems in the design of more effective chemotherapeutic agents. To enhance the clinical utility of future generations of therapeutic agents, lead compounds will need to carry out homing assignments such as the targeting of tissues, the penetration into cells, and the routing to specific organelles. The refinement of prototypic agents for achieving such a spectrum of functions continues to be a difficult task. An alternate strategy has been to develop immunotoxins or related conjugates which can target a cytotoxic function to cancer cells. However, these constructs are structurally complex protein platforms for which parameters such as their penetration into tumors (*3*−*5*) as well as their intracellular routing and processing remain poorly understood (*6, 7*). The concept of loligomers[1] (*8*) has recently been developed as a design strategy for creating multitasking agents. Loligomers (derived from the Latin root *loligo* referring to members of the squid family) are assemblies of small functional domains presented on a tentacular scaffold to increase the number and exposure of domains. The structure of loligomers highlights the following features: a scaffold of lysine residues giving rise to a branched peptide presenting multiple domains that code for functions such as cellular delivery, cell signaling, and/or cytotoxicity. These constructs can be synthesized rapidly using automated approaches in solid phase peptide synthesis. Loligomer 4 in particular can spontaneously penetrate into

† This work was supported by a grant from the National Cancer Institute of Canada with funds from the Canadian Cancer Society. D.S. was the recipient of successive AMGEN and George Knudson Foundation fellowships during the work on this project. E.C.L. was the recipient of a fellowship from the Medical Research Council of Canada.

* To whom correspondence should be addressed at Ontario Cancer Institute, Princess Margaret Hospital, 610 University Ave., Toronto, Canada M5G 2M9. Phone: (416) 946-2967. Fax: (416) 946-6529. E-mail: gariepy@oci.utoronto.ca.

[1] Abbreviations: CTS, cytoplasmic translocation signal; loligomer, squid-like branched peptide construct that incorporates cell penetration and intracellular localization signals; loligomer 4, loligomer harboring eight N-terminal arms that comprise a pentalysine cytoplasmic translocation domain and the SV40 large T-antigen nuclear localization signal; loligomer 4Rh, variant of loligomer 4 derivatized at its single thiol arm with tetramethylrhodamine; MFI, mean fluorescence intensity as derived by flow cytometry; NLS, nuclear localization signal; NPC, nuclear pore complex; RLU, relative light unit.

[2] This structure represents a variant of the original loligomer 4 construct (*8*) where the C-terminal sequence Tyr-Gly-βAla was substituted with the tetrapeptide Cys-Gly-Tyr-βAla to permit the introduction of thiol-reactive probes.

S0006-2960(97)02762-1 CCC: $15.00
Published on Web 04/09/1998

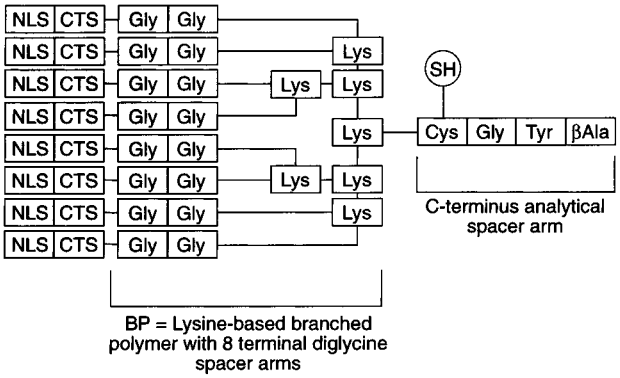

FIGURE 1: Structure of loligomer 4, a peptide-based intracellular vehicle (*8*) that is able to penetrate eukaryotic cells and self-localize in the nucleus. It consists of a five-amino acid, C-terminal region (analytical arm) and eight identical N-terminal arms linked together through a branched lysine polymer (BP). Each N-terminal arm contains a domain representing the nuclear localization signal of the SV40 large T-antigen residues 124−135 (NLS, Thr-Pro-Pro-Lys-Lys-Lys-Arg-Lys-Val-Glu-Asp-Pro; *34*) and a lysine pentapeptide acting as a cytoplasmic translocation signal (CTS). The thiol side chain on the cysteine residue incorporated in the analytical arm was derivatized with either a fluorescent tetramethylrhodamine group (loligomer 4Rh) or a biotin moiety (loligomer 4Biotin).

cells and self-localize in the nucleus (*8*; Figure 1).[2] In this report, we analyzed the penetration and intracellular migration of one such loligomer, termed loligomer 4, into eukaryotic cell lines in an effort to define the broadness and extent of their localization properties based on initial design premises. The data suggest that the construct can import large molecular entities such as plasmids and is found in vesicles, the cytosol, and the nucleus of cells.

EXPERIMENTAL PROCEDURES

Peptide Synthesis. The construction of defined branched peptides by solid phase peptide synthesis was first developed by Tam (*9*, *10*). The branched peptide (loligomer 4) was synthesized on an Applied Biosystems 430A Synthesizer using *tert*-butoxycarbonyl (t-Boc) chemistry and a phenylacetamidomethyl (PAM) resin support (*11*). The synthesis, coupling efficiencies, purification, and characterization procedures were described previously (*8*). The structure of loligomer 4 is presented in Figure 1 and highlights a cysteine residue at the fourth position of its C terminus (analytical arm). The thiol group at this site was derivatized with maleimido-containing agents to introduce either a fluorescent probe (tetramethylrhodamine) or a biotin moiety. Briefly, the thiol group was initially reduced by dissolving 1 mg of loligomer 4 in 100 μL of sodium borate buffer (pH 9.1) and adding 100 μL of 0.1 M $NaBH_4$ in borate buffer. The sample tube was placed on ice, and the reduction step was left to proceed for 15 min. The solution was acidified with 20 μL of 6 N HCl (pH 2) and then quickly readjusted to pH 6.0 with 5 N NaOH. Tetramethylrhodamine was incorporated into the reduced thiol group of loligomer 4 by adding 0.1 mg of tetramethylrhodamine 5(6′)-maleimide (Molecular Probes, Eugene, OR) dissolved in 0.1 M citrate buffer (pH 6.5) to the loligomer 4 solution. The resulting solution was stirred overnight at 4 °C. The excess rhodamine reagent was removed by size exclusion chromatography using a Sephadex G-25 column (30 cm × 1 cm outside diameter) equilibrated in phosphate-buffered saline (PBS). The molar ratio of rhodamine fluorophore incorporated into loligomer 4 was <1, and the resulting compound was termed loligomer 4Rh.

Biotin maleimide (0.7 mg, Molecular Probes) was dissolved in 100 μL of dimethylformamide and the mixture added dropwise to a 1 mg solution of reduced loligomer 4 (in an ~225 μL volume adjusted to pH 6.0; as described in the previous paragraph). The content of the reaction vessel was gently mixed overnight at 4 °C. The excess biotin reagent was removed by size exclusion chromatography using a Sephadex G-25 column (30 cm × 1 cm outside diameter) equilibrated in phosphate-buffered saline (PBS). The presence of the biotin group on the construct was confirmed by ELISA. Briefly, wells of 96-well plates were coated for 1 h at room temperature with 0.5 μg of the desalted biotinylated peptide. Nonspecific sites were then blocked with 0.1% (w/v) BSA in PBS (200 μL, 1 h at room temperature), and the wells were further treated with streptavidin−horseradish peroxidase (200 μL prepared in PBS, 1 h at room temperature; dilutions from 1:2000 up to 1:10000). The washing solution contained 0.1% (w/v) BSA in PBS. The presence of biotin as monitored by the increase in absorbance at 405 nm [using 2,2′-azinobis(3-ethylbenzthiazoline-6-sulfonic acid) as the substrate; Sigma, St. Louis, MO] was not detected in wells coated with loligomer 4 but was easily observed in wells harboring the biotinylated derivative (results not shown). The resulting compound was termed loligomer 4Biotin.

Cell Lines and Culture Conditions. The following cell lines were routinely grown at 37 °C and in 5% CO_2 in growth medium consisting of α-MEM supplemented with 10% (v/v) fetal bovine serum (ImmunoCorp, Montreal, Canada), penicillin (1 unit/mL), streptomycin (100 μg/mL), and 1 mM glutamine: EL-4 (murine T-cell lymphoma; *12*), Daudi (human Burkitt's lymphoma; *13*, *14*), MCF-7 (human breast carcinoma; *15*), VERO (African green monkey kidney cells; *16*), COS-7 (SV40 transformed African green monkey kidney cells; *17*), and CHO (Chinese hamster ovary cells subclone AUXB1; *18*). These cells were grown as adherent monolayers or in suspension (with stirring) in spinner glass flasks.

Cytotoxicity Assays. A cell viability assay was used to determine the toxicity of loligomer 4Rh toward CHO, EL-4, and MCF-7 cells. The colorimetric assay is based on the cleavage of the tetrazolium salt WST-1 [Boehringer Mannheim, Montreal, Canada; 4-[3-(4-iodophenyl)-2-(4-nitrophenyl)-2*H*-5-tetrazolio]-1,3-benzene disulfonate] to its formazan by a mitochondrial succinate−tetrazolium reductase system active only in viable cells (*19*, *20*). The tritiated thymidine incorporation assay (*21*−*23*) was employed to monitor the proliferation of COS-7, Daudi, MCF-7, and VERO cells in the presence of loligomer 4Rh. Briefly, 10^4 cells suspended in growth medium were seeded in 96-well plates and incubated for 4 h at 37 °C with increasing concentrations of loligomer 4Rh (1 μM to 1 mM). For the WST-1 assay, cells with the peptide-containing medium were incubated for 4 h at 37 °C and the medium was replaced with 200 μL of fresh medium containing WST-1 (10 μL/well). The orange formazan product was quantified by measuring the optical density of the cell extract at 450 nm. Absorbance values were translated into measurements of cell viability, representing the average of triplicate wells and experiments performed at least three times. For the tritiated

thymidine assay, the peptide-containing medium in each well was replaced with thymidine (Td) deficient α-MEM (100 μL/well) containing [^{3}H]Td (1 μCi/well). Cells were maintained overnight at 37 °C in a humidified 5% CO_2 incubator. Adherent cells were then harvested by treating them with a trypsin−trypsin-EDTA solution. One milliliter of scintillation fluid was added to each tube containing harvested cells on filters. Counts per minute (cpm) values derived from at least three different experiments performed in triplicate were converted into percentage units of cell proliferation in relation to untreated cells.

Flow Cytometry. CHO cells (10^6 cells) were exposed to 0.1 μM loligomer 4Rh prepared in growth medium. At selected time intervals, cells were washed with PBS and resuspended in sample buffer (PBS). Cellular uptake (37 °C) and cell surface association (4 °C) of loligomer 4Rh were analyzed on a FACScan unit (Becton Dickinson, San Jose, CA). Cytometric data were analyzed for viable cells only by adding the membrane impermeant fluorescent DNA intercalator 7-aminoactinomycin D (7-AAD, 0.1 mg/mL; *24*, *25*) to cells just prior to flow cytometry and by subsequently gating data collection to record cells showing high forward scatter values and low 7-AAD fluorescence intensities. Experiments were performed in triplicate with 10 000 or more events being recorded.

Fluorescence and Confocal Microscopy. CHO cells were grown either as a monolayer, in suspension in a spinner flask (with constant stirring), or as a suspension of freshly trypsinized cells cultured originally as a monolayer. Cell preparations were subsequently exposed to 0.1 μM loligomer 4Rh dissolved in growth medium. At selected time intervals, a sample (10^6 cells) of each cell preparation was recovered by centrifugation, resuspended in a growth medium containing acridine orange (1 mM), and incubated for 5 min at room temperature. Cells were washed three times with PBS, centrifuged, and resuspended in fresh PBS. A drop of unfixed cells was deposited directly on a microscope slide and examined by fluorescence microscopy (Nikon, Fluor100/1.3 oil) or by confocal fluorescence microscopy (Zeiss LSM410 instrument). A standard fluorescein excitation filter was used for observing the acridine orange signal (Nikon, 480/520 filter), and a rhodamine filter (Nikon, BA590 filter) was used to observe the rhodamine signal from loligomer 4Rh. Digital imaging was used to construct merged images from confocal microscopy (*26*). Mean intensity values (per pixel) were derived from confocal images of CHO cells using the software program NIH Image (version 1.61). Values were averaged over more than 50 sections defining the cytosol or nuclei of five separate images of CHO cell preparations pretreated with loligomer 4Rh.

Electron Microscopy. CHO cells, derived from culturing them either as monolayers or in suspension (spinner flask, 10^6 cells/mL), were incubated for 4 h in the presence or absence of loligomer 4Biotin (0.1 μM) previously prepared in growth medium. Cells were harvested and placed into a fixative solution (5% glutaraldehyde/PBS) for 4 h at 20 °C. The samples were then cooled to 4 °C, washed with PBS buffer, stained [1% (w/v) OsO_4 in cacodylate buffer (pH 7.4)], dehydrated in ethanol, and embedded in epoxy resin (TAAB Laboratories, Buffalo, NY). Thin sections were cut and deposited onto copper and/or nickel grids. Sections were washed with 1% (w/v) BSA in PBS for 5 min and treated for 30 min with 25 μL droplets of either a 1:10 or 1:20 dilution of a 15 nm colloidal gold−streptavidin conjugate (British Biocell International, Cardiff, U.K.) dissolved in PBS. The grids were then washed once with 1% (w/v) BSA in PBS and five times with sterile distilled water droplets (50 μL) for 10 min. The sections were finally stained with uranyl acetate and Reynold's lead citrate (successive 5 min staining steps) and visualized by transmission electron microscopy (Hitachi H600 microscope). The distribution of gold particles present in the nucleus and cytoplasm of cells was determined by visually counting particles from electron micrograph negatives. Nucleus:cytoplasm ratios were calculated by dividing the total number of particles within the areas of the cytoplasm and the nucleus. More than 20 micrographs of CHO cells were analyzed for particle distribution for grids treated with the colloidal gold−streptavidin solution.

Disruption of Cytoskeletal Components. Monolayers of CHO cells were treated for 1 h with either 0.3 μM cytochalasin D (*Zygusporium monsonii*; Calbiochem, San Diego, CA) or 0.125 μM colchicine (*Colchicum autumnale*; Calbiochem) and subsequently exposed to 0.1 μM loligomer 4Rh dissolved in growth medium. In a second series of experiments, these inhibitors were added to the medium of CHO cells at the same time as loligomer 4Rh. At selected time intervals, cells were washed, resuspended in PBS buffer, and analyzed by flow cytometry. The morphology of CHO cells was also verified by light microscopy. Initial experiments were performed to identify the optimal noncytotoxic concentration of drugs able to cause the phenotypic rounding of CHO cells.

Transfection of Plasmid−Loligomer 4Rh Complexes. Loligomer 4Rh (ranging from 1 to 60 μg prepared in PBS) was mixed with 10 μg of either plasmid pGL2 luciferase (Promega, Madison, WI) or pCMV βgal (Clontech, Palo Alto, CA). Sample volumes were then adjusted to 50 μL with PBS, and the mixtures were incubated at room temperature for 5 min. At a ratio of 1 μg of loligomer 4Rh per microgram of plasmid, a complete shift to higher masses was observed in the migration pattern of plasmids in agarose gels (results not shown). CHO cells (2×10^5 cells) in growth medium were then added to the plasmid−loligomer 4Rh preparations, giving a final volume of 500 μL. The cell suspensions were incubated on a rotor or shaker at 37 °C in an Eppendorf tube for up to 5 h. The cells were subsequently plated in a six-well dish with an additional 4 mL of growth medium for 48 h. In the case of cells transfected with the plasmid construct harboring the luciferase reporter gene, the luciferase activity was monitored by harvesting the treated cells in 200 μL of lysis buffer (Promega) and by disrupting them using a single 5 min freeze−thaw cycle (−70 to 37 °C). Cell supernatants were collected by centrifugation (8000 rpm, 5 min). Aliquots (20 μL) of each cell lysate were then mixed with 100 μL of a luciferase substrate solution (Promega) and luminescence units recorded in a luminometer (Lumat LB 9507, Berthold, Princeton, NJ). The protein concentration of each cell lysate was determined using a dye binding assay (Bio-Rad, Hercules, CA), and the total amount of luciferase activity was reported in terms of light units per milligram of protein in the extracts. Each bar in the histogram presented in Figure 8 represents the average of three or more experiments, each performed in

duplicate. The expression of β-galactosidase in cells transfected with either the pCMV βgal plasmid alone or in a complex with loligomer 4Rh was detected using 5-bromo-4-chloro-3-indolyl β-D-galactoside (X-gal) as the histochemical substrate (*27*). Briefly, transfected cells were rinsed twice with PBS. Cells were overlaid with 0.75% (v/v) glutaraldehyde, incubated at 37 °C for 5 min, and subsequently washed three times with PBS. The resulting fixed cells were then overlaid with a X-gal staining solution [100 mM sodium phosphate (pH 7.3), 1.3 mM $MgCl_2$, 3 mM $K_3Fe(CN)_6$, 3 mM $K_4Fe(CN)_6$, and 1 mg/mL X-gal] and incubated for a period of 12−24 h at 37 °C. The staining solution was aspirated, and cells were washed with PBS prior to being visualized under bright field microscopy.

RESULTS AND DISCUSSION

Design and Synthesis of Loligomer 4 Variants. Loligomers (*8*) are peptide-based shuttles able to deliver a signal, inhibitor, or cytotoxic functionality to an intracellular site. The concept of loligomers evolved from the realization that future drug design strategies will have to provide effective solutions for selectively delivering cytotoxic or therapeutic agents to the cytosol or inside cellular compartments. The term loligomer emphasizes the branched or "squid-like" nature of these peptides and was derived from the Latin root *loligo* referring to members of the squid family. In particular, loligomer 4 (Figure 1) contains eight nuclear localization signals (NLS) and eight pentalysine stretches acting as cytoplasmic translocation signals (CTS) which allow it to penetrate cells and relocate to their nuclei, the site of action of several classes of therapeutic agents. The construction of branched peptides as opposed to the use of linear sequences stems from the concept that a multivalent display of functional domains leads to high binding avidity and enhanced functional activity. Multivalency is the dominant feature of other recent delivery strategies based on dendrimers (*28*−*30*) and peptabodies (*31*). For example, it has been demonstrated that, in the case of protein conjugates, the efficiency of their nuclear targeting property increases with the number of NLS sequences coupled to them (*32*, *33*). In addition, the branched nature of loligomers gives them advantages compared to linear peptides in terms of incorporating or positioning tissue-targeting sequences and cytotoxic moieties. Finally, branching reduces the impact of proteolytic degradation on loligomers since all arms would need to be cleaved to block their localization properties. The experimental focus of this study was to evaluate cellular parameters affecting the import and localization of loligomer 4 inside eukaryotic cells. Loligomer 4 (Figure 1) was assembled by classical approaches in solid phase peptide synthesis (see Experimental Procedures). Branching was introduced following successive rounds of couplings of lysine derivatives harboring identical protecting groups on their α- and ϵ-amino groups. This synthetic approach was developed by Tam (*9*, *10*) for the creation of multiple antigenic peptides. The eight arms of loligomer 4 are identical and include the well-characterized nuclear localization signal (NLS) of the SV40 large T antigen (Thr-Pro-Pro-Lys-Lys-Lys-Arg-Lys-Val-Glu-Asp-Pro; *34*) as well as five consecutive lysines that act as cytoplasmic translocation signals (CTS). The display of eight pentalysine sequences on loligomer 4 results in a construct that possesses the cellular import properties of linear, high-molecular weight polylysine chains (*35*−*38*). A single cysteine residue was inserted between the first branching lysine of the polymer and a glycine residue in the C-terminal analytical arm. Two variants of loligomer 4 were created by derivatizing the resulting thiol side chain with either a spectrofluorometric probe or a biotin group; loligomer 4Rh incorporates a fluorescent rhodamine chromophore for flow cytometry and fluorescence microscopy, while the biotinylated derivative termed loligomer 4Biotin was used in electron microscopy studies.

Eukaryotic Cells Are Sensitive to Micromolar Concentrations of Loligomer 4Rh. Loligomer 4 was not engineered to carry cytotoxic groups. However, our previous study had shown that such molecules are moderately cytotoxic toward Chinese hamster ovary (CHO) cells in the absence of any cytotoxic moieties. Notably, linear polymers of polylysine have also been shown to possess cytotoxic properties (*37*). The cytotoxicity of loligomer 4Rh toward six mammalian cell lines was investigated to assess the generality of this phenomenom. It was also essential to determine the appropriate loligomer 4Rh concentration for detecting its rhodamine signal by flow cytometry and fluorescence microscopy in viable cells. The following cell lines were selected for our studies on the basis of their ability to be monitored by flow cytometry and fluorescence microscopy as well as for the ease of growing these cells as monolayers or in suspension: a murine T-cell lymphoma cell line (EL-4), a human Burkitt's lymphoma cell line (Daudi), a human breast carcinoma cell line (MCF-7), an African green monkey kidney cell line (VERO), a SV40-transformed African green monkey kidney cell line (COS-7), and a Chinese hamster ovary cell line (CHO). One of two assays was used to determine the toxicity of loligomer 4Rh toward these cell lines: either a cell viability assay based on the cellular generation of a colored formazan derivative (WST-1; *19*, *20*) or a cell proliferation assay based on the incorporation of tritiated thymidine during DNA synthesis as a measure of cell growth (*21*−*23*). The choice of the assay was a function of the cell line examined. For example, the incorporation of tritiated thymidine into CHO and EL-4 cells was marginal. Thus, the effect of the loligomer 4Rh concentration on the viability of CHO, MCF-7, and EL-4 cells was determined using the WST-1 assay (Figure 2A), while the proliferation of COS-7, MCF-7, Daudi, and VERO cells was measured using the tritiated thymidine assay (Figure 2B). The toxicity of loligomer 4Rh toward MCF-7 cells was evaluated using both assays for a comparison. Loligomer 4Rh was found not to be toxic to any of the cell lines tested at concentrations below 5 μM. Twenty to fifty percent of cells remain viable when exposed to a 100 μM concentration of the construct for 20 h at 37 °C, except for EL-4 and Daudi cells which did not survive doses above 60 μM. Loligomer 4Rh and loligomer 4Biotin were used at a concentration of 0.1 μM (well below CD_{50} values) for subsequent uptake and localization studies.

Loligomer 4Rh Uptake into Eukaryotic Cells. Loligomer 4Rh incorporates a fluorescent rhodamine probe that allows one to monitor the uptake of loligomers into cells by flow cytometry. Two important variables relating to the penetration of loligomer 4Rh into viable cells were investigated at a concentration of loligomer 4Rh considered nontoxic to cells

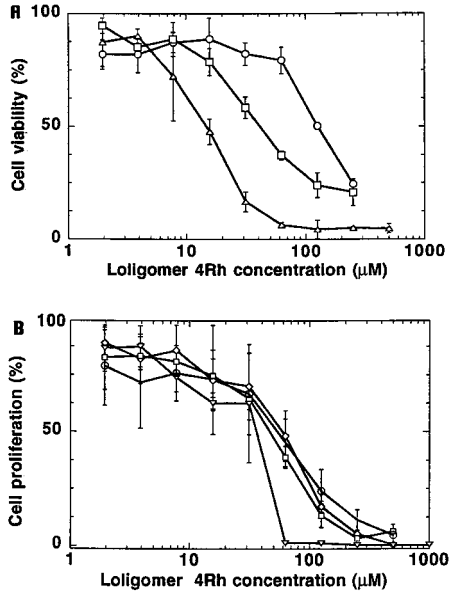

FIGURE 2: Cytotoxicity of loligomer 4Rh toward established eukaryotic cell lines. The effect of the loligomer 4Rh concentration on the survival of six cell lines was determined by exposing cells to this construct for 4 h at 37 °C. Cell proliferation was measured by the incorporation of tritiated thymidine, while cell viability was assessed using a colorimetric assay (WST-1). The toxicity of loligomer 4Rh toward the cell line MCF-7 was measured using both assays to establish a comparison between them. Both assays yielded similar loligomer 4Rh CD_{50} values of ~40 μM for MCF-7 cells. (A) Effect of the loligomer 4Rh concentration on cell viability as measured by a colorimetric assay based on the cleavage of the tetrazolium salt WST-1 in viable cells: ○, CHO; □, MCF-7; and △, EL-4. (B) Effect of the loligomer 4Rh concentration on cell proliferation as measured by the incorporation of tritiated thymidine: ◇, COS-7; □, MCF-7; ○, VERO; and ▽, Daudi.

(0.1 μM). Can growth conditions (temperature, suspension cells versus adherent cells) affect the mechanisms of loligomer uptake, and does the level of cellular import depend on cell types? The incorporation of pentalysine sequences into loligomer 4 stems from the observation that the composition of the outer membrane leaflet present on the surface of most eukaryotic cells tends to confer a net negatively charged surface to cells which favors their interactions with polylysine (*39*) and the cellular uptake of cationic molecules. We have demonstrated that the presence of eight cationic CTS domains (pentalysine stretches; Figure 1) favors the penetration of loligomer 4Rh into cells by absorptive endocytosis (*8*). This process is arrested at low temperatures. Thus, when cells are incubated at 4 °C, one should only observe the association of loligomer 4Rh to cell surface components. Correspondingly, the amount of loligomer 4Rh (in terms of mean fluorescence intensities or MFIs) bound to the surface of all six cell lines tested in the present study was small or negligible (Figure 3) when loligomer 4Rh was incubated with cells at 4 °C over a period of 6 h. The most dramatic uptake levels occurred when cell lines were grown in suspension at 37 °C. Cell lines such as VERO and COS-7 (both African green monkey kidney cell lines) showed a striking uptake of this loligomer with MFI values reaching 5×10^2 to 10^3 after 6 h. CHO (Chinese hamster ovary) and MCF-7 (human breast cancer) cells imported the construct very well (MFIs of >200 at 6 h), while Daudi (human B cell lymphoma) and EL-4 (murine lymphoma) cell lines (two cell lines that normally grow in suspension) internalized the construct weakly (MFIs of ~20 at 6 h). All six cell lines were able to internalize the construct when grown in suspension (Figure 3; as confirmed by flow cytometry and fluorescence microscopy). The uptake of the construct by many cell lines did not show an initial burst, and the process of cellular internalization appears to plateau within 6 h.

The penetration of loligomer 4Rh into viable cells grown as adherent monolayers at 37 °C was significantly reduced in relation to cells maintained in suspension. COS-7 and MCF-7 cells demonstrated diminished but reasonable levels of loligomer 4Rh import (120−180 MFIs), while VERO and CHO cells reached modest uptake values on the order of 60 MFIs after 6 h (Figure 3A−D). EL-4 and Daudi cells normally exist in suspension. Both cell lines were allowed to deposit and attach weakly to wells for this experiment but showed little uptake of the construct (Figure 3E,F). A clear distinction between adherent cells and cells grown in suspension is their morphology, being rounded in suspension and adopting extended, multifaceted shapes as cells composing a monolayer. Does the rounded morphology of a cell grown in suspension represent a manifestation of an altered cytoskeleton that favors the uptake of loligomers? Since cell shape is defined by cytoskeletal components, we investigated the use of inhibitors of cytoskeletal networks to monitor this parameter. Microtubules and actin filaments have been linked to vesicular transport. Cytochalasins prevent the polymerization of actin filaments causing fibroblasts to "round up" and actin bundles to contract. Microtubule assembly inhibitors such as colchicine bind to tubulin dimers and thereby block the polymerization of tubulin. Cytochalasin D and colchicine were used to verify if the cytoskeleton does, in any way, alter the uptake of loligomer 4Rh into the cytoplasm or nuclei of CHO cells. No significant increase in loligomer 4Rh uptake was observed in the case of CHO cell monolayers pretreated for 1 h with cytochalasin D (0.3 μM) prior to the addition of the construct (0.1 μM) (results not shown). Similarly, the treatment of cells with colchicine (0.125 μM) showed no effect on loligomer uptake whether cells were treated initially with colchicine or incubated along with loligomer 4Rh (results not shown). The absence of effect by this drug on loligomer import was observed for CHO cells either maintained as monolayer cells, trypsinized, or grown as suspension cells in a spinner flask. Thus, a severe disruption of microfilament (actin) or microtubule (tubulin) networks in CHO cells did not result in an increase in loligomer uptake. Cellular parameters other than cytoskeletal fiber networks may differentiate cells growing in suspension from cells cultured as monolayers.

The cytotoxicity of loligomer 4Rh toward eukaryotic cells (Figure 2) does not correlate with the ability of cells to internalize the construct in viable cells (Figure 3). The clearest examples are the Daudi and EL-4 cell lines which are the most sensitive cell lines to loligomer 4Rh concentrations yet represent the cell lines least able to import the construct. This fact may have to do with the composition of the cell surface and a possible role of loligomers in destabilizing cell membranes at high concentrations causing cell death. Alternatively, as cells accumulate and retain high levels of such cationic species (loligomer 4Rh) and their associated counterions, the intracellular concentration of

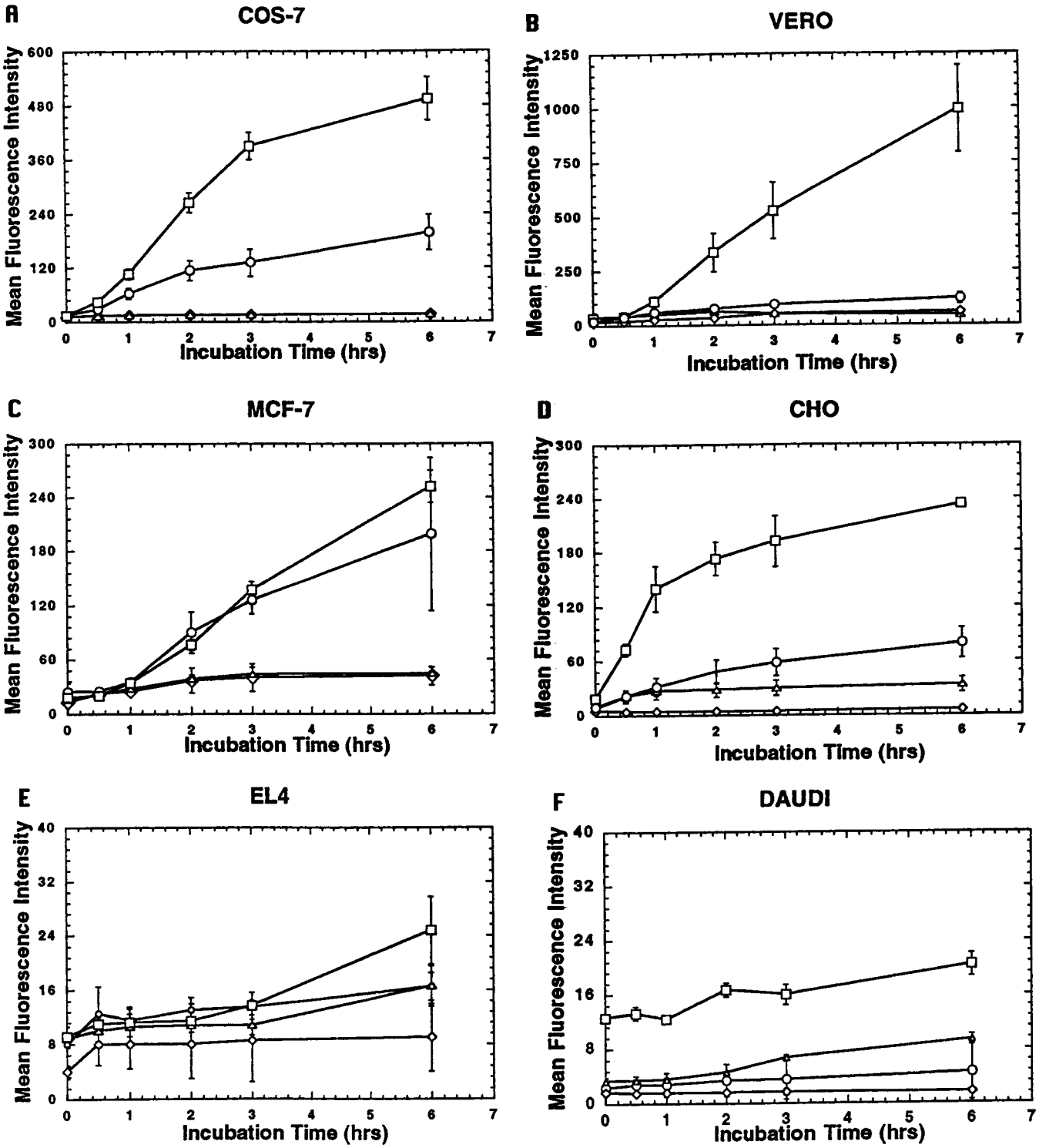

FIGURE 3: Cellular uptake of loligomer 4Rh by mammalian cells. Mean fluorescence intensities of cells exposed to a 0.1 μM solution of loligomer 4Rh as a function of incubation time, cell presentation (suspension vs monolayer), and temperature (4 and 37 °C): (A) COS-7 cells, (B) VERO cells, (C) MCF-7 cells, (D) CHO cells, (E) EL-4, and (F) Daudi cells. Cells were maintained as monolayer cells at (◇) 4 °C and (○) 37 °C or in suspension at (△) 4 °C and (□) 37 °C.

solutes increases, causing water to move continuously into the cell by osmosis.

Loligomer 4Rh Is Irreversibly Retained Inside Cells. A major issue in the intracellular delivery of loligomers is establishing if the processes leading to cytoplasmic uptake and nuclear import are cumulative and nonreversible. As presented in Figure 3, the uptake of loligomer 4Rh starts to plateau for most cell lines within 6 h of exposure to the construct. It was recently demonstrated, using flow cytometry, that the extent of loligomer 4Rh uptake by CHO cells was proportional to its extracellular concentration (*8*; D. Singh and J. Gariépy, unpublished observations) up to micromolar concentrations where one starts to observe a significant level of loligomer cytotoxicity toward all cell lines tested (Figure 2). More importantly, the process of loligomer internalization appears to be irreversible. CHO cells were incubated at 37 °C with loligomer 4Rh (0.1 μM) for 4 h in suspension. After the growth medium containing the con-

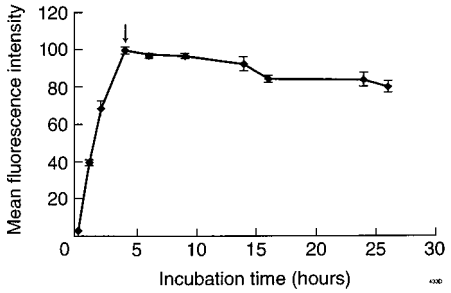

FIGURE 4: Cellular retention of loligomer 4Rh by CHO cells. Mean fluorescence intensities of CHO cells exposed to a 0.1 μM solution of loligomer 4Rh as a function of incubation time. The growth medium containing loligomer 4Rh was exchanged with fresh medium after incubating cells for 4 h at 37 °C (arrow). Flow cytometry measurements were performed over a time interval of 26 h.

struct was removed and replaced with fresh medium, the rhodamine signal was monitored as a function of time by flow cytometry (Figure 4). Ninety percent (90%) of the fluorescence signal persisted 14 h postincubation with 80% of the signal still retained by CHO cells after 25 h. The examination of cell preparations by fluorescence microscopy showed that, following the wash step, the fluorescence signal in the cytosol of CHO cells slowly diminished (on the scale of hours) while loligomer 4Rh remained or accumulated predominantly in the nuclei of these cells. Some of the rhodamine fluorescence signal was still faintly visible in the cytoplasm of CHO cells, 24 h following the wash step (results not shown). Previous studies (*8*; J. Sheldon and J. Gariépy, unpublished observations) had shown that the rhodamine tag comigrates with loligomers inside cells (using a loligomer with dual fluorescence labels on all N-terminal and C-terminal arms) and that degradation of loligomers was not significant during the time scale of our experiments (using D- vs L-amino acid containing loligomers). In summary, a large proportion of internalized loligomer 4Rh does not cycle out of CHO cells, suggesting that retention mechanisms, particularly the nuclear import process, may irreversibly sequester the construct in the nuclei of cells.

Visualization of Loligomer Internalization and Nuclear Localization. The major differences in cytoplasmic uptake observed between cell lines (Figure 3) suggest that more than one possible transport event may be operating. This conclusion is supported by the fact that the design of loligomer 4 codes for internalization and nuclear uptake signals, but lacks a signal allowing its translocation out of vesicular compartments. Yet nuclear uptake requires the transient passage of the construct to the cytosol. It was thus essential to visualize the routing of this construct into cells.

The multiple locations of loligomer 4 inside cells were defined by electron microscopy. The biotinylated construct loligomer 4Biotin in conjunction with streptavidin−gold (15 nm particles) was used to reveal its cellular location in CHO cells (Figure 5). Electron micrographs clearly prove for the first time the presence of loligomer 4 in vesicular compartments (Figure 5B,C; endocytic vesicles) as well as confirm

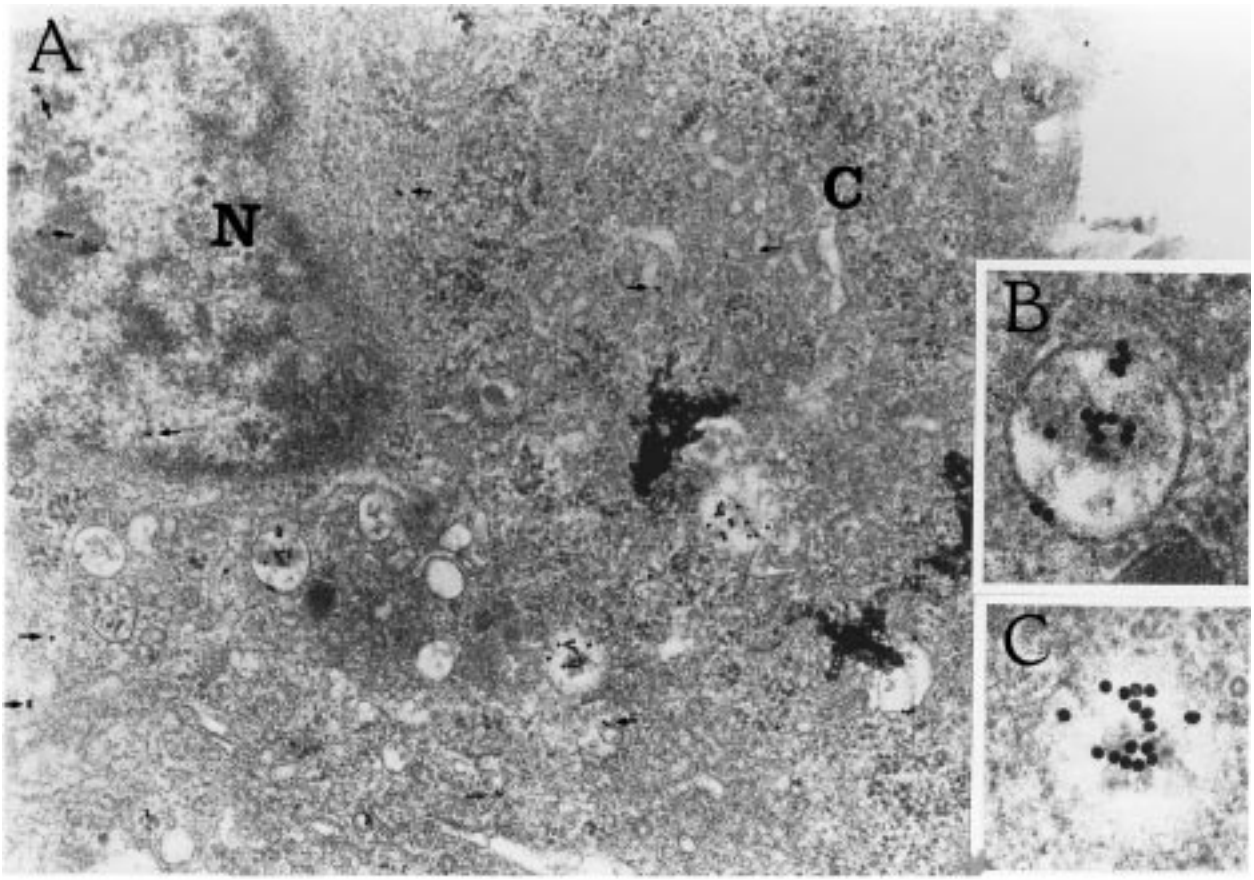

FIGURE 5: Migration of loligomer 4Biotin into viable CHO cells as monitored by electron microscopy. Micrographs of CHO cells exposed to a 0.1 μM solution of loligomer 4Biotin for 4 h at 37 °C. The cellular routing of loligomer 4Biotin was monitored by incubating fixed CHO cells with colloidal streptavidin gold particles. (A) Gold particles (15 nm, arrows) were visible in both the nucleus (N) and cytosol (C) of CHO cells. (B and C) Magnifications of vesicular compartments observed in A, which contained clusters of gold particles. Magnifications of the electron micrograph were (A) 46 400 times and (B and C) 95 700 times.

its location in the cytosol and in the nuclei of cells (Figure 5A). The semiquantitative tabulation of gold particles found in the nuclei and cytoplasm of CHO cells in the presence or absence of loligomer 4Biotin provides an estimate of the localization potential of the construct inside cells. The distribution of gold particles in these two compartments was individually derived by counting particles observed in at least 20 micrographs of CHO cells initially exposed to the construct. The average particle numbers in the same compartments derived from a control set of electron micrographs of untreated CHO cells were then subtracted from the total particle counts recorded in the two compartments for loligomer 4Biotin-labeled CHO cells. The number of particles associated with background readings typically represented 20−30% of values tabulated for micrographs of CHO preparations exposed to loligomer 4Biotin. Gold labeling of loligomer 4Biotin was performed at two final protein concentrations of the streptavidin−gold particle conjugate. At a streptavidin−colloidal gold particle dilution of 2.2 μg of protein/mL, 97 ($\pm$13) particles were found in the nuclei (*N*) of CHO cells as opposed to 38 ($\pm$2) in the cytosol (*C*), giving an *N*/*C* ratio of 2.5; at a dilution of 1.1 μg of protein/mL, 29 ($\pm$1) particles were found in the cytoplasm of CHO cells and 31 ($\pm$14) in their nuclei for an *N*/*C* ratio of 1.1. Since the surface area of the nucleus typically occupies ~25% of a CHO cell in a thin section (please refer to Figure 6 for the relative dimensions of the nuclear compartment in a typical CHO cell), one can assume that the cytoplasm occupies an area at least 3 times the size of the nucleus. The *N*/*C* ratios of gold particles as a function of surface area would thus emphasize the actual increased accumulation of loligomer 4Biotin in the nuclei of CHO cells in relation to the cytosol, and these values can be approximated by simply multiplying the *N*/*C* ratios by a factor of ~3. This calculation suggests that the level of loligomer 4Biotin in the nucleus significantly exceeds its cytoplasmic concentration by at least a factor ranging between 3 (3×1.1) and 7 (3×2.5). Reconstructed images derived from confocal microscopy of CHO cells treated with loligomer 4Rh also confirm the presence of the loligomer 4 in the cytosol and nuclei of CHO cells (Figure 6). Within the first hour of incubation, loligomer 4Rh was rapidly internalized by CHO cells maintained in suspension and was clearly visible in the nucleus by 4 h (Figure 6). Acridine orange is a cationic dye that stains nucleic acid-containing areas in CHO cells (Figure 6A, in green), while rhodamine fluorescence detects the presence of loligomer 4Rh (Figure 6B, in red). Confocal images were processed to depict the colocalization of both chromophores (Figure 6C). Yellow-colored areas observed when both images are combined represent cellular regions accessed by both dyes. Again, the nuclei of CHO cells qualitatively accumulate more of the loligomer than the cytoplasmic area. Optical sections (thickness of 0.5 μm) were also performed on cell preparations by confocal microscopy and confirmed the localization of loligomer 4Rh in a large proportion of cell nuclei (results not shown). Averaged intensity values (per pixel) were recorded from randomly selected sections of the cytoplasm and nuclei derived from a representative set of five labeled CHO cell images. The averaged *N*/*C* ratio observed over all cell compartments measured was 2.3 ± 0.5, indicating that loligomer 4Rh selectively accumulated in the nuclei of these cells.

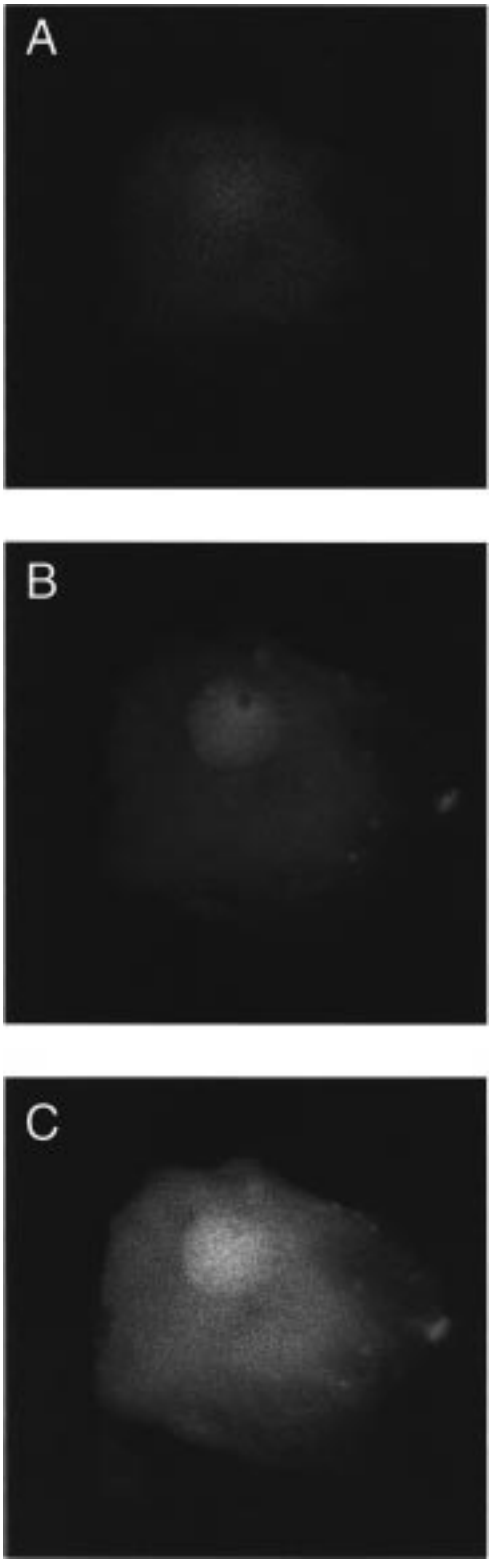

FIGURE 6: Penetration and localization of loligomer 4Rh inside viable CHO cells after a 4 h incubation at 37 °C. The migration of loligomer 4Rh bearing rhodamine groups was monitored by confocal microscopy. Fluorescence photographs were recorded on an unfixed, viable preparation of CHO cells. Fluorescence images were recorded for (A) DNA content in the cells with the nucleic acid stain acridine orange, (B) loligomer 4Rh content with rhodamine, and (C) a confocal converged image of acridine orange and rhodamine.

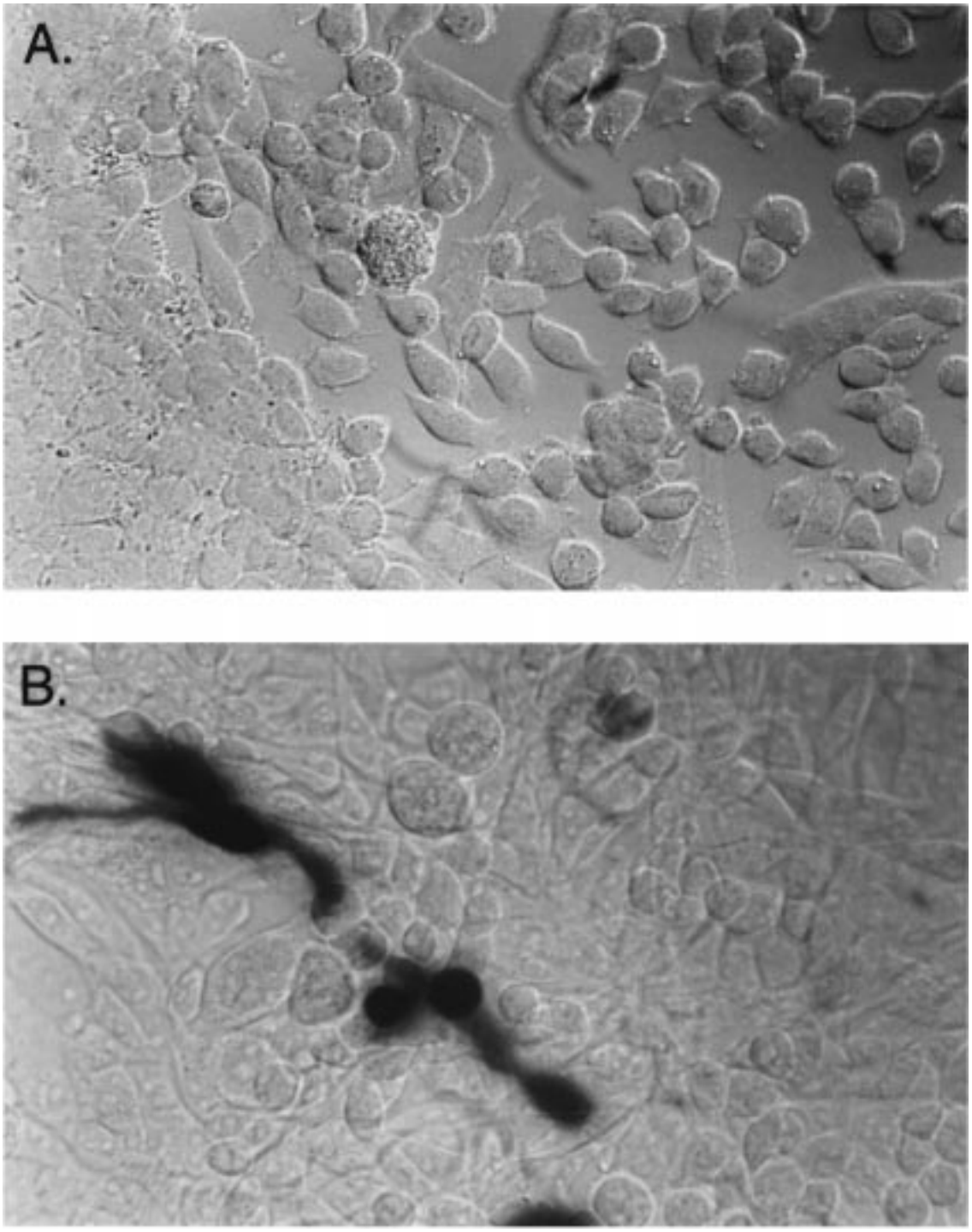

FIGURE 7: Expression of β-galactosidase in CHO cells transfected with loligomer 4 complexed to a plasmid harboring a β-galactosidase reporter gene. CHO cells (2×10^5 cells) were exposed to a mixture containing the plasmid pCMV β-gal (10 μg) and loligomer 4 (30 μg). (A) CHO cells treated with the plasmid alone show no indigo staining of cells, an event indicative of the hydrolysis of the substrate X-gal by β-galactosidase. (B) Indigo-colored cells are observed in a field of CHO cells after treatment with the plasmid−loligomer 4 complex.

Loligomers Can Shuttle Noncovalently Associated Plasmids to the Nuclei of Cells. Can loligomers deliver large molecular entities such as proteins or plasmids into cells? Functional assays associated with the use of plasmids carrying reporter genes can be employed to monitor their delivery to the nuclei of cells by loligomers. Experimentally, the plasmids pGL2 luciferase or pCMV βgal were individually mixed with loligomer 4Rh to generate noncovalently bound complexes. The resulting macromolecular aggregates are easily observed as high-molecular weight species on agarose gels. Their noncovalent association is due to the fact that loligomer 4Rh is a cationic structure that can readily interact with the negatively charged phosphate backbone of plasmid DNA. The exposure of CHO cells to plasmid−loligomer 4Rh complexes resulted in the efficient expression of both genes and their respective gene products, namely, luciferase and β-galactosidase. For example, the expression of β-galactosidase as a result of transfecting CHO cells with the pCMV βgal plasmid−loligomer 4 complex was revealed using the substrate 5-bromo-4-chloro-3-indolyl β-D-galac-

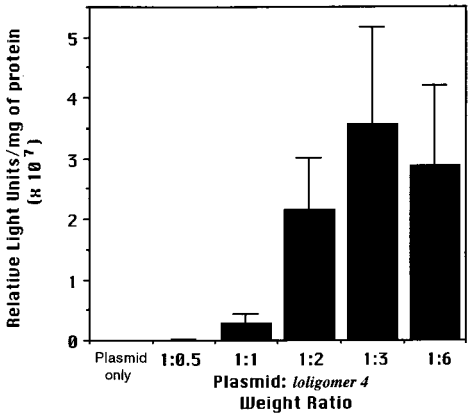

FIGURE 8: Luciferase activity present in CHO cells transfected with a complex of loligomer 4 and a plasmid containing a luciferase gene reporter construct. The pGL2 luciferase plasmid (10 μg) was complexed with increasing amounts of loligomer 4 (5−60 μg) and added to a suspension of CHO cells (2×10^5 cells). Cells were harvested in a lysis solution (200 μL), and the level of luciferase activity present in lysates was measured and reported as relative light units per milligram of protein (RLU/mg, as described in Experimental Procedures). The addition of the plasmid alone to CHO cells yielded no detectable level of luciferase activity.

toside (X-gal) which produces an indigo precipitate (Figure 7). Only the plasmid−loligomer 4 complex yielded the expression of β-galactosidase in these cells (Figure 7B) as opposed to cells exposed to the plasmid alone (Figure 7A). Similarly, the import and nuclear localization of the pGL2 luciferase vector complexed to loligomer 4Rh into CHO cells were confirmed by monitoring the extent of luciferase activity present in the cytosol of transfected cells. The histogram presented in Figure 8 highlights the level of luciferase activity (per milligram of protein) in CHO cell extracts as a function of the weight ratio of plasmid to loligomer 4Rh used to initially transfect CHO cells. The efficiency of the transfection event was dramatic at weight ratios between 1:1 and 1:6. In summary, large molecular entities such as plasmids can be transported by loligomers into viable cells, and the resulting complexes can self-localize into the nucleus, leading to the transcription and/or translation of reporter genes.

Model Explaining the Routing of Loligomer 4 into Cells. Loligomer 4 was designed to carry signals to be endocytosed by cells and to be shuttled to the nuclei of cells. An early step in the nuclear import of proteins requires that NLS-containing proteins interact with cytosolic carrier molecules such as α-importin (*40*−*42*). Consequently, loligomers 4 must gain access to the cytosol. Electron and fluorescence microscopy images suggest the presence of loligomer 4 variants in the cytosol, vesicular compartments, and the nuclei of cells. No signals have been incorporated into these structures that would allow their translocation across vesicular membranes. An intracellular routing model is proposed in Figure 9 to explain the fact that loligomers alone (Figures 5 and 6) or associated with plasmids (Figures 7 and 8) can reach the nuclei of cells. The model suggests the uptake of loligomers by absorptive endocytosis (*1*) and their presence in the cytosol prior to nuclear transport via the nuclear pore complex. The present model emphasizes the entrapment of loligomers in vesicles as a dominant compartment accessed by them during cellular trafficking. The destabilization of such vesicles is proposed as the mechanism by which loligomers are translocated to the cytosol. No evidence presently supports the occurrence of such an event, except for the fact that loligomers are observed in the cytoplasm soon after the cells are exposed to them (Figures 5 and 6). Loligomers may have membrane-active properties which may destabilize vesicular compartments, leading to their leakage into the cytosol. Indeed, a recent report by Zauner and co-workers (*43*) suggests that polylysine in the presence of glycerol can lyse internal vesicles. An alternate model could be proposed where loligomer 4 enters cells via two penetration mechanisms, one involving vesicular compartments (in agreement with the electron microscopy data) and another unknown mechanism which would place loligomer 4 directly into the cytosol. Loligomers entrapped in vesicles would be trafficked in and out of the cell, while loligomers accessing the cytosol directly would be efficiently transported to the nucleus. This second model however would necessitate the transient passage of loligomers across the plasma membrane. Trypan blue staining of cells during their exposure to loligomer 4Rh indicates that the dye does not transiently cross the plasma membrane (results not shown). Thus, the integrity of the cell membrane is retained during loligomer treatment (0.1 μM). Second, we do not observe a significant loss of loligomer from cells after removing the construct from the medium (Figure 4), suggesting that the recycling of loligomers to the surface of cells and their subsequent release into the medium via vesicular transport do not represent a dominant exocytosis pathway. In summary, the routing of loligomer 4Rh into cells is best described by the model presented in Figure 9.

Enhanced Avidity and the Presentation of Functional Domains Are Key Features of Loligomers. The long-term objective of loligomer research is to provide a structural platform for designing simple peptide-based multitasking agents that may aid in the development of therapeutic agents. Our initial efforts have focused on evaluating the penetration and trafficking of one such loligomer prototype (loligomer 4), which incorporates multiple copies of the nuclear localization signal (NLS) of the SV40 large T-antigen as well as pentalysine sequences acting as cytoplasmic translocation signals (CTS). The reason for targeting the nuclei of cells stems from the fact that this compartment represents the intracellular site of action of common classes of chemotherapeutic agents known to disrupt the structure of DNA or its replication. In the future, cell specificity can be introduced into such constructs by identifying small peptide ligands able to bind specifically to cancer cells using phage-display and synthetic peptide libraries, as exemplified by the S peptide specific for the mouse B-cell lymphoma BCL1 (*31*).

Loligomers are branched peptides that were designed to provide multiple arms with the view of augmenting the avidity of synthetic constructs for binding to cells or for enhancing their ability to self-localize inside cells. The potential of branched peptides as agents that are able to target tissues and cells was typified by the polymerization of a short peptide derived from the B1 chain of laminin, Tyr-Ile-Gly-Ser-Arg (YIGSR), and its ability to inhibit tumor growth and metastasis (*44*). Although sequences as common as cell adhesion domains of laminin or fibronectin may lack specificity for tumor cells, this study (*44*) supports the concept that the use of branching peptides for presenting

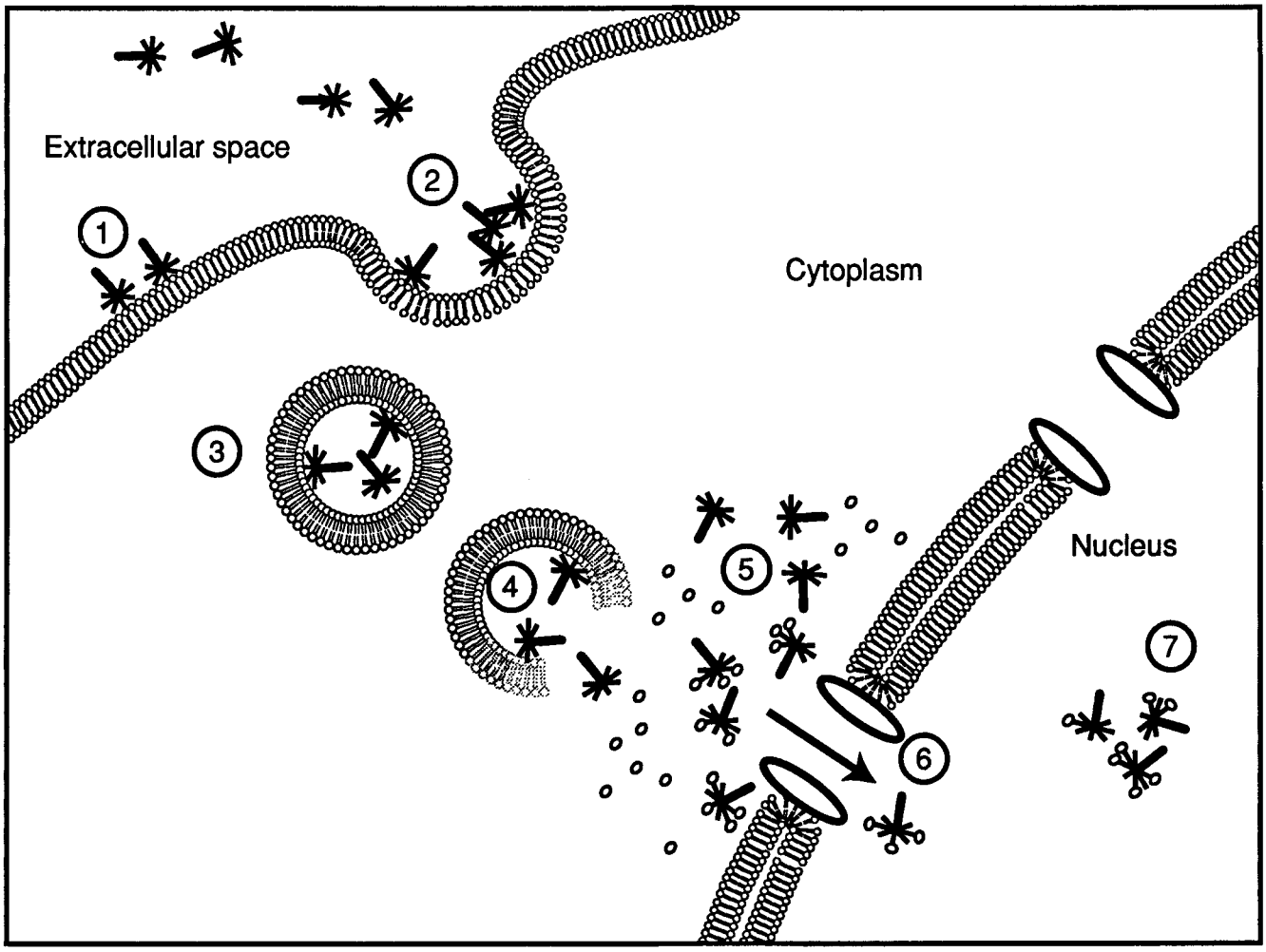

FIGURE 9: Proposed routing of loligomer 4 into a eukaryotic cell. Loligomers 4 (dark tentacular structures) initially bind to membrane surface components (anionic sites) and are taken up into vesicular compartments by absorptive endocytosis (stages 1−3). A fraction of the compartmentalized construct escapes to the cytosol (stage 4) where their nuclear localization signals are recognized by cytosolic carriers (open circles, stage 5). These complexes are then imported into the nucleus (stage 6). Loligomer 4 molecules are retained in this compartment (stage 7).

multiple copies of weak adhesion domains may result in constructs that harbor an enhanced avidity for cell surface receptors.

In addition to the need to generate more specific chemotherapeutic agents, it is important to introduce more potent cytotoxic agents into loligomer constructs. Indeed, a guided delivery of a cytotoxic agent should result in a significant decrease in the number of molecules needed (CD_{50} dose) to delete a cell. Interestingly, linear peptides incorporating an internalization sequence derived from *Antennapedia* fused to $p21^{WAF1}$ peptides have been designed to block cell growth. However, these optimized constructs possess only moderate cell growth inhibitory activities toward two human ovarian cancer cell lines with IC_{50} values on the order of 30−300 μM (*45*). These linear peptides can be contrasted with loligomer 4 constructs which are cytotoxic at those concentrations and have yet to incorporate cytotoxic functionalities. Photodynamic probes, antisense sequences, and metal chelators as well as plasmids can now be attached to loligomers 4 (on multiple arms during solid phase assembly) or noncovalently associated with them to target the nuclei of cells, with the view of enhancing their cytotoxic properties. These observations emphasize the fact that a multivalency of functional domains represents an important factor in enhancing both the uptake and cytotoxicity of loligomer 4 in relation to strategies involving linear peptides.

ACKNOWLEDGMENT

The authors thank Steven Doyle and Battista Calvieri for their kind help with electron and confocal microscopy, Jim Ferguson for synthesizing peptides, Juliet Sheldon for her technical assistance in operating the flow cytometer, and Drs. Mark Bray and Davinder Chawla for their critical evaluation of the manuscript.

REFERENCES

1. Gallop, M. A., Barrett, R. W., Dower, W. J., Fodor, S. P. A., and Gordon, E. M. (1994) *J. Med. Chem. 37*, 1233−1251.
2. Gordon, E. M., Barrett, R. W., Dower, W. J., Fodor, S. P. A., and Gallop, M. A. (1994) *J. Med. Chem. 37*, 1385−1401.
3. Juweid, M., Neumann, R. D., Palk, C., Perez-Bacete, M. J., Sato, J., van Osdol, W., and Weinstein, J. N. (1992) *Cancer Res. 52*, 5144−5153.
4. Shockley, T. R., Lin, K., Nagy, J. A., Tompkins, R. G., Yarmush, M. L., and Dvorak, H. F. (1992) *Cancer Res. 52*, 367−376.
5. Saga, T., Neumann, R. D., Heya, T., Sato, J., Kinuya, S., Le, N., Paik, C. H., and Weinstein, J. N. (1995) *Proc. Natl. Acad. Sci. U.S.A. 92*, 8999−9003.

6. Blakey, D. C., Wawrzynczak, E. J., Wallace, P. M., and Thorpe, P. E. (1988) in *Monoclonal Antibody Therapy* (Waldmann, H., Ed.) pp 50−90, Karger, Basel, Switzerland.
7. Yazdi, P. T., Wenning, L. A., and Murphy, R. M. (1995) *Cancer Res. 55*, 3763−3771.
8. Sheldon, K., Liu, D., Ferguson, J., and Gariépy, J. (1995) *Proc. Natl. Acad. Sci. U.S.A. 92*, 2056−2060.
9. Tam, J. P. (1988) *Proc. Natl. Acad. Sci. U.S.A. 85*, 5409−5413.
10. Tam, J. P. (1989) *Methods Enzymol. 168*, 7−15.
11. Stewart, J. M., and Young, J. D. (1984) *Solid Phase Peptide Synthesis*, 2nd ed., Pierce, Rockford, IL.
12. Moore, M. W., Carbone, F. R., and Bevan, M. J. (1988) *Cell 54*, 777−785.
13. Klein, E., Klein, G., Nadkarni, J. J., Wigzell, H., and Clifford, P. (1968) *Cancer Res. 28*, 1300−1310.
14. Nilsson, K., Giovanella, B. C., Stehlin, J. S., and Klein, G. (1977) *Int. J. Cancer 19*, 337−344.
15. Soule, H. D., Vazquez, J., Long, A., Albert, S., and Brennan, M. (1973) *J. Natl. Cancer Inst. 51*, 1409−1416.
16. Rhim, J. S., and Schell, K. (1967) *Nature 216*, 271−272.
17. Gluzman, Y. (1981) *Cell 23*, 175−182.
18. McBurney, M. W., and Whitmore, G. F. (1974) *Cell 2* (3), 173−182.
19. Slater, T. F., Sawyer, B., and Strauli, U. (1963) *Biochim. Biophys. Acta 77*, 383−393.
20. Mosmann, T. J. (1983) *Immunol. Methods 65*, 55−63.
21. Bradley, L. M. (1980) in *Selected Methods in Cellular Immunology* (Mishell, B. B., and Shiigi, S. M., Eds.) pp 153−172, W. H. Freeman and Company, New York.
22. Biorchi, V., and Fortunati, E. (1990) *Toxicol. in Vitro 4*, 9−16.
23. Shevach, E. M. (1994) in *Current Protocols in Immunology* (Coligan, J. E., Kruisbeek, A. M., Margulies, D. H., Shevach, E. M., and Strober, W., Eds.) Vol. 3, John Wiley & Sons, New York.
24. Gill, J. E., Jotz, M. M., Young, S. G., Modest, E. J., and Sengupta, S. K. (1975) *J. Histochem. Cytochem. 23*, 793−799.
25. Zelenin, A. V., Poletaev, A. I., Stepanova, N. G., Barsky, V. E., Kolesnikov, V. A., Nikitin, S. M., Zhuze, A. L., and Gnutchev, N. V. (1984) *Cytometry 5*, 348−354.
26. Paddock, S. W., Hazen, E. J., and De Vries, P. J. (1997) *BioTechniques 22*, 120−126.
27. MacGregor, G. R., Nolan, G. P., Fiering, S., Roerderer, M., and Herzenberg, L. (1991) in *Methods in Molecular Biology−Gene Transfer and Expression Protocols* (Murray, E. J., Ed.) pp 217−235, Humana Press, Clifton, NJ.
28. Kukowska-Latallo, J. F., Bielinska, A. U., Johnson, J., Spindler, R., Tomalia, D. A., and Baker, J. R., Jr. (1996) *Proc. Natl. Acad. Sci. U.S.A. 93*, 4897−4902.
29. Bielinska, A. U., Kukowska-Latallo, J. F., Johnson, J., Tomalia, D. A., and Baker, J. R., Jr. (1996) *Nucleic Acids Res. 24*, 2176−2182.
30. Zimmerman, S. C., Zeng, F., Reichert, D. E. C., and Kolotuchin, S. V. (1996) *Science 271*, 1095−1098.
31. Terskikh, A. V., LeDoussal, J.-M., Crameri, R., Fisch, I., Mach, J.-P., and Kajava, A. V. (1997) *Proc. Natl. Acad. Sci. U.S.A. 94*, 1663−1668.
32. Roberts, B. L., Richardson, W. D., and Smith, A. E. (1987) *Cell 50*, 465−475.
33. Dworetzky, S. I., Lanford, R. E., and Feldherr, C. M. (1988) *J. Cell Biol. 107*, 1279−1287.
34. Kalderon, D., Richardson, W. D., Markham, A. F., and Smith, A. E. (1984) *Nature 311*, 33−38.
35. Shen, W.-C., and Ryser, H. J.-P. (1978) *Proc. Natl. Acad. Sci. U.S.A. 75*, 1872−1876.
36. Shen, W. C., and Ryser, H. J.-P. (1979) *Mol. Pharmacol. 16*, 614−622.
37. Arnold, L. J., Jr., Dagan, A., Gutheil, J., and Kaplan, N. O. (1979) *Proc. Natl. Acad. Sci. U.S.A. 76*, 3246−3250.
38. Leonetti, J.-P., Degols, G., and Lebleu, B. (1990) *Bioconjugate Chem. 1*, 149−153.
39. Ryser, H. J. P., Drummond, I., and Shen, W. C. (1986) in *Targeting of drugs with synthesis systems* (Gregoriadis, G., Senior, J., and Poste, G., Eds.) pp 103−121, Plenum Publishing Co., New York.
40. Adam, S. A., Marr, R. S., and Gerace, L. (1990) *J. Cell Biol. 111*, 807−816.
41. Gorlich, D., Vogel, F., Mille, A. D., Hartmann, E., and Laskey, R. A. (1995) *Nature 377*, 246−248.
42. Mahajan, R., Delphin, C., Guan, T., Gerace, L., and Melchior, F. (1997) *Cell 88*, 97−107.
43. Zauner, W., Kichler, A., Schmidt, W., Mechtler, K., and Wagner, E. (1997) *Exp. Cell Res. 232*, 137−145.
44. Nomizu, M., Yamamura, K., Kleinman, H. K., and Yamada, Y. (1993) *Cancer Res. 53*, 3459−3461.
45. Bonfanti, M., Taverna, S., Salmona, M., D'Incalci, M., and Broggini, M. (1997) *Cancer Res. 57*, 1442−1446.

BI972762L